ACADEMIC PRESS

Available online at www.sciencedirect.com

SCIENCE DIRECT®

Experimental Neurology 182 (2003) 21–34

Experimental Neurology

www.elsevier.com/locate/yexnr

Neuronal and glial pathological changes during epileptogenesis in the mouse pilocarpine model

Karin Borges,[a,*] Marla Gearing,[b] Dayna L. McDermott,[a] Amy B. Smith,[a] Antoine G. Almonte,[a] Bruce H. Wainer,[b] and Raymond Dingledine[a]

[a] *Department of Pharmacology, Emory University, Atlanta, GA 30322, USA*
[b] *Department of Pathology and Laboratory Medicine, Emory University, Atlanta, GA 30322, USA*

Received 16 November 2002; revised 6 February 2003; accepted 19 February 2003

Abstract

The rodent pilocarpine model of epilepsy exhibits hippocampal sclerosis and spontaneous seizures and thus resembles human temporal lobe epilepsy. Use of the many available mouse mutants to study this epilepsy model would benefit from a detailed neuropathology study. To identify new features of epileptogenesis, we characterized glial and neuronal pathologies after pilocarpine-induced status epilepticus (SE) in CF1 and C57BL/6 mice focusing on the hippocampus. All CF1 mice showed spontaneous seizures by 17–27 days after SE. By 6 h there was virtually complete loss of hilar neurons, but the extent of pyramidal cell death varied considerably among mice. In the mossy fiber pathway, neuropeptide Y (NPY) was persistently upregulated beginning 1 day after SE; NPY immunoreactivity in the supragranular layer after 31 days indicated mossy fiber sprouting. β2 microglobulin-positive activated microglia, normally absent in brains without SE, became abundant over 3–31 days in regions of neuronal loss, including the hippocampus and the amygdala. Astrogliosis developed after 10 days in damaged areas. Amyloid precursor protein immunoreactivity in the thalamus at 10 days suggested delayed axonal degeneration. The mortality after pilocarpine injection was very high in C57BL/6 mice from Jackson Laboratories but not those from Charles River, suggesting that mutant mice in the C57BL/6(JAX) strain will be difficult to study in the pilocarpine model, although their neuropathology was similar to CF1 mice. Major neuropathological changes not previously studied in the rodent pilocarpine model include widespread microglial activation, delayed thalamic axonal death, and persistent NPY upregulation in mossy fibers, together revealing extensive and persistent glial as well as neuronal pathology.

Keywords: Epilepsy; Seizure; Microglia; Astrocyte; Neuropeptide Y; Neurodegeneration; Axonal degeneration; β2 Microglobulin; Amyloid precursor protein; Hippocampus; Thalamus

Introduction

The induction of status epilepticus (SE) by pilocarpine or kainate in rodents leads to a series of neuropathological changes and the subsequent appearance of spontaneous recurrent seizures (epilepsy). Many features of the rodent models, such as hippocampal sclerosis and mossy fiber sprouting, resemble human temporal lobe epilepsy. The rat pilocarpine model is commonly used in epilepsy research and has been well characterized (e.g., Cavalheiro et al., 1991; Mello et al., 1993; Turski et al., 1983). In contrast, the mouse pilocarpine model has received much less attention, although the availability of mice harboring mutations or deletions of many genes offers the opportunity to study the role of these genes in neurodegeneration and epileptogenesis. Neurodegeneration and development of spontaneous recurrent seizures (SRS) following pilocarpine injections in albino Swiss mice were first reported in 1984 (Turski et al., 1984) , and a few groups have studied the mouse pilocarpine model since then in different strains, such as albino (Cavalheiro et al., 1996), CD1 (Shibley and Smith, 2002), and

* Corresponding author. Department of Pharmacology, Emory University School of Medicine, 1510 Clifton Road, Atlanta, GA 30322. Fax +1-404-727-0365.
E-mail address: kborges@pharm.emory.edu (K. Borges).

0014-4886/03/$ – see front matter © 2003 Elsevier Science (USA). All rights reserved.
doi:10.1016/S0014-4886(03)00086-4

C57BL/6 obtained from Harlan (Shibley and Smith, 2002) or from Charles River (Berkeley et al., 2002) . Both rats and mice show hilar and pyramidal cell loss, astrogliosis, and mossy fiber sprouting after pilocarpine-induced SE in the hippocampus. Moreover, severe cell damage was found in other brain regions, such as amygdala and thalamus (Turski et al., 1984).

Although neuronal cell loss, astrogliosis, and mossy fiber sprouting have been described in the mouse and rat pilocarpine model, many other neuropathological events in the latent period during epileptogenesis have not been studied to date. In the present study we focused on the time course of changes in activation of microglial cells, expression of neuropeptide Y (NPY), and axonal degeneration in CF1 and C56BL/6 mice to gain insight into potential mechanisms in the development of epilepsy. We report widespread microglial activation, persistent NPY upregulation in the mossy fiber pathway, and delayed axonal degeneration in the thalamus. We found unexpectedly large differences in pilocarpine-induced mortality in C57BL/6 mice obtained from different suppliers, a factor that may limit the usefulness of these mice for studies of epileptogenesis.

Methods

Animals and treatment

Mice were obtained from Charles River (CF1, C57BL/6(Charles River)) or Jackson Laboratories (C57BL/6(JAX)) and housed under a 12-h light–dark cycle with food and water ad libidum. CF1 mice (6–10 weeks old, 30–42 g), C57BL/6 (JAX) (6–15 weeks old, 17–32 g, or >1 year old and 21–32 g), and C57BL/6 (Charles River) mice (10-weeks old, 21–25 g) were used. To minimize peripheral side effects of pilocarpine, mice were injected with methylscopolamine and terbutaline 15–30 min prior to pilocarpine (2 mg/kg each ip in 0.9% NaCl). Different doses of a single ip injection of pilocarpine (in 0.9% NaCl) were required to induce SE in the different mouse strains: 254–290 mg/kg for CF1, 247–335 mg/kg for C57BL/6 (JAX), and 300–315 mg/kg for C57BL/6 (Charles River) mice "Uninjected" mice received terbutaline and methylscopolamine but no pilocarpine (n = 3–4 uninjected mice at each time point). All drugs were obtained from Sigma.

Seizures were classified according to Racine (1972) and Schauwecker and Steward (1997) with slight modifications: normal activity (stage 0); rigid posture or immobility (stage 1); stiffened, extended, and often arched (Straub) tail (stage 2); partial body clonus, including forelimb or hindlimb clonus (seen rarely) or head bobbing (stage 3); whole body continuous clonic seizures while retaining posture (stage 3.5); rearing (stage 4); severe whole body continuous clonic seizures while retaining posture (stage 4.5); rearing and falling (stage 5); and tonic–clonic seizures with loss of posture or jumping (stage 6). SE was defined by continuous seizure activity for at least 2 h consisting of at least stage 3.5 seizures and one stage 5 or 6 seizure or several stage 4.5 seizures. CF1 mice were filmed during SE and the number of stage 5 and 6 seizures occuring over a 5-6-h period following pilocarpine injection was counted to estimate the severity of SE.

SE was terminated by injection of 30 mg/kg pentobarbital (Sigma) in all C57BL/6 (JAX) mice after 1, 2, 2.5, or 4.5 h of SE, and in 11 of 13 C57BL/6 (Charles River) mice after 4.5 h of SE. Two C57BL/6 (Charles River) and all CF1 mice received no pentobarbital and behavioral seizures subsided after about 5 h. After SE, all mice were injected with 0.5–0.8 ml 5% dextrose in lactate Ringer solution ip. Mice were fed moistened high-fat rodent chow and were monitored daily and injected with 5% dextrose in lactate Ringer solution when needed. Mice typically lost 18% of body weight during SE, and weight stayed relatively low over the following 4 weeks (6% lower weight at 31 days relative to weight at day of injection). Mice euthanized after 31 days were videotaped on several days for 1.5–6 h per day. A person blinded to the treatment analyzed videotapes for the occurrence of spontaneous stage 4–6 seizures. All experiments were approved by the Institutional Animal Care and Use Committee of Emory University and conducted in accordance with its guidelines. Every effort was made to minimize animal suffering.

Neuropathology

Mice were euthanized under deep flurothane anesthesia at different time points, and brains were removed and immersed in 4% paraformaldehyde fixative for at least 10 h. Brains were sliced coronally in 1- to 2-mm slices, dehydrated in a graded series of alcohols and xylenes, and infiltrated with paraffin using an automated tissue processor (Shandon Hypercenter XP), and then embedded in paraffin blocks. Eight-micrometer sections were cut using a Shandon AS325 microtrome, and every 10th section was stained with hematoxylin. Healthy neurons could be easily distinguished from nonneuronal cells and injured neurons by their large size, medium-intensity staining, and dark nucleoli (see Figs. 1A2, inset, and 4G, arrowheads). After SE, pyramidal cells often were shrunken and stained darkly (pyknotic cells, e.g., see Fig. 1B2, arrowheads) or had disappeared at late time points (e.g., Fig. 1C).

The amount of hippocampal pyramidal damage in pilocarpine-treated versus uninjected mice was assessed between −1.8 and −2.5 mm bregma (corresponding to mid-level hippocampal sections according to the atlas for C57BL/6 mice in Hof et al. (2000) by a blinded investigator. The same investigator (K.B.) conducted all subjective ratings. The amount of damage in the hippocampal pyramidal CA1 (all sectors considered together) and CA3 regions (all sectors considered together), and the whole pyramidal cell layer, were scored for each mouse on a 0–4 scale, by estimating in 25% increments the number of healthy cells

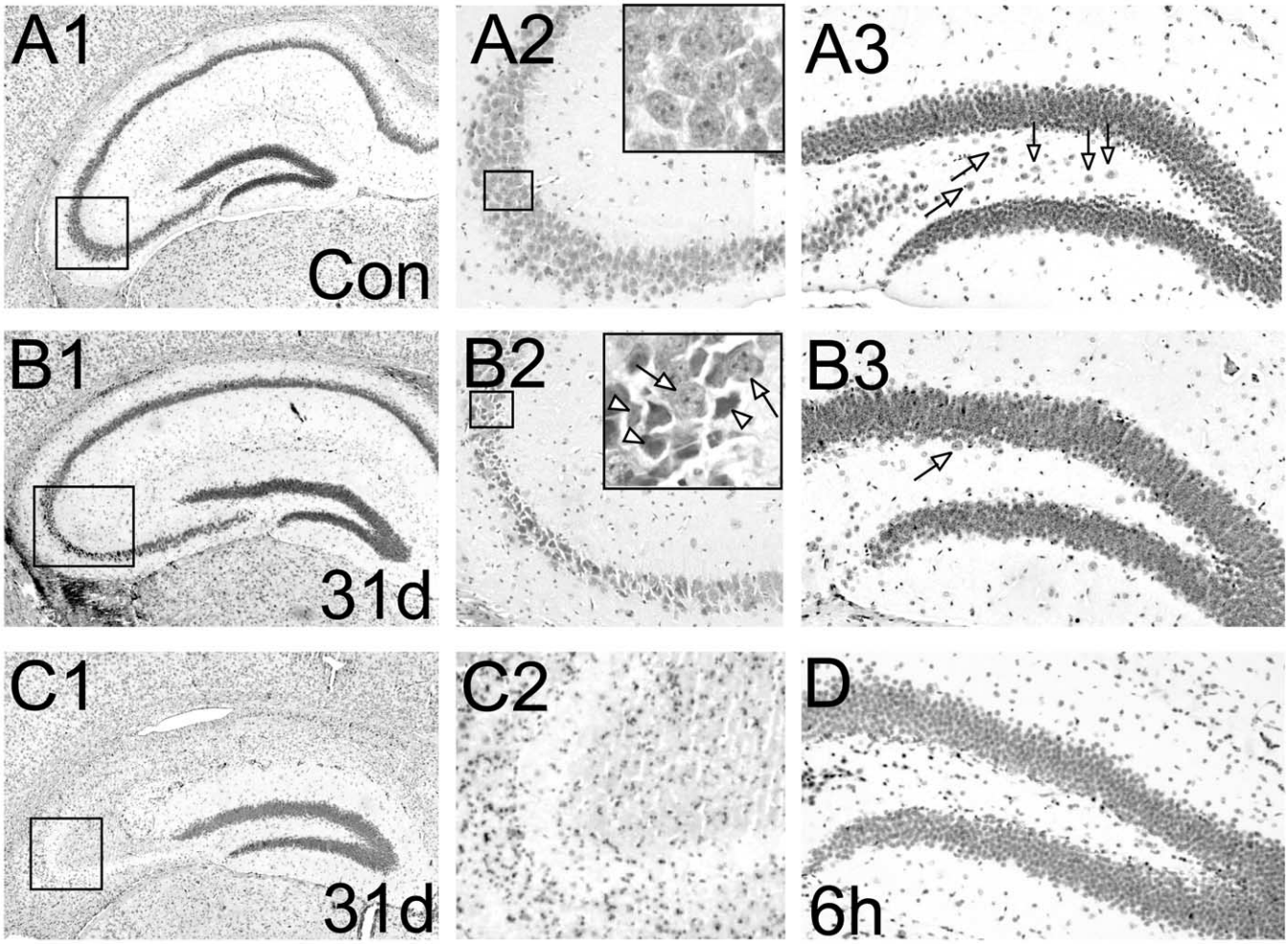

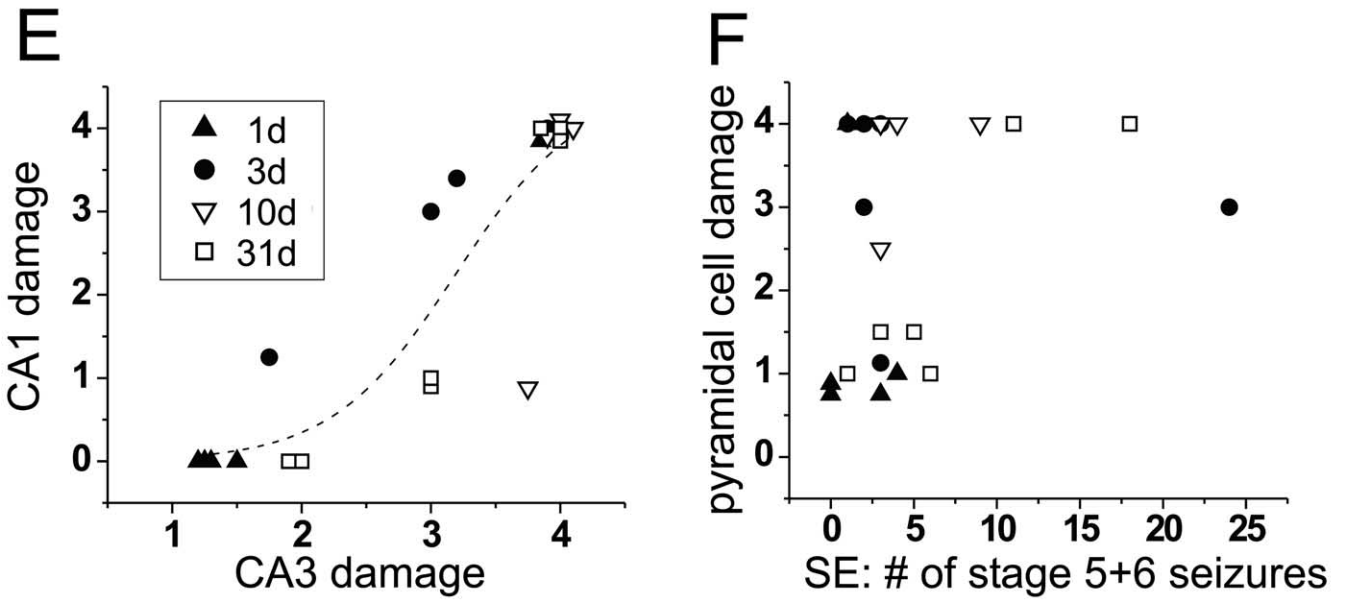

Fig. 1. Hippocampal damage in the pilocarpine mouse model. (A) Hematoxylin-stained 8-μm sections showing the hippocampus (A1), part of the CA3 region (A2), and the hilus (A3) of an uninjected mouse. The inset in A2 shows a high magnification of typical healthy pyramidal cells with noticeable nucleoli. Arrows in A3 point to hilar neurons. (B) Comparable sections from a mouse 31 days after SE with pyknotic neurons in the CA3b (B2) area but normal histology in CA1 (total damage score, 1). The inset of B2 shows a high magnification of pyknotic cells (arrowheads) and healthy neurons in the same field (arrows). (B3) The hilus exhibited near-complete loss of neurons (arrow points to the only healthy hilar neuron in this section). (C) Sections from a mouse at 31 days with frank loss of pyramidal cells (total damage score, 4). (D) The hilus of a mouse euthanized 6 h after SE showing complete loss of hilar neurons. (E) Damage scores in CA3 and CA1 pyramidal cell layers are plotted with a fitted curve for all 1 to 31-day mice that experienced SE. The time of euthanasia after SE is indicated by different symbols (inset). (F) The total pyramidal damage score (same mice and same symbols as in E) is plotted against the severity of SE estimated by the number of stage 5 and 6 seizures experienced during SE.

Table 1
Pretreatments, dilutions, and incubation conditions for all primary antibodies used

Primary antibody	Source	Dilution	Incubation	Pretreatment
Rabbit anti-cow GFAP	Dako Corp.	1:500	40°C for 30 min	None
Rat anti-mouse F4/80	Serotec	1:25	4°C for 24 h	Pepsin
Rabbit anti-rat/human NPY	Peninsula Laboratories	1:500	4°C for 24 h	Microwave
Human APP mAb	Boehringer Mannheim	1:200	4°C for 24 h	Microwave
Goat anti-mouse β2 microglobulin (M20)	Santa Cruz Biotechnology	1:200	4°C for 24 h	Formic acid

Note. Pretreatments were performed as follows: incubation for 10 min at 40°C with pepsin reagent (Biomeda Corp.), incubation for 10 min at room temperature with 90% formic acid, or sections were microwaved twice at highest power for 5 min in 100 ml 10 mM citric acid (pH 6.0).

remaining relative to uninjected mice. Score 0 was given if the section was undistinguishable from control mice, i.e., the number of healthy neurons appeared normal, even if a few pyknotic cells were found. Score 1, >75% healthy pyramidal cells remaining, but with clear evidence of cell death (e.g., Fig. 1B); 2, 50–74%; 3, 25–49%; 4, <25% healthy pyramidal neurons remaining (e.g., Fig. 1C). The median score was calculated for each mouse from at least three hippocampal sections at different levels. The number of hilar cells was counted in the hippocampus in two to nine sections from each mouse at −2.1 to −2.4 mm from bregma.

Immunohistochemistry

Eight-micrometer-thick paraffin-embedded sections were immunohistochemically labeled as described (Gearing et al., 1993). Briefly, sections were deparaffinized in a series of xylenes and graded alcohols and were blocked with normal serum and then incubated with primary antibody, followed by biotinylated secondary antibody and avidin–biotin–peroxidase complex (ABC Elite Kit; Vector Laboratories, Burlingame, CA). For the F4/80 antibody only, the Dako Envision System (DAKO Corporation, Carpinteria, CA) was used as instructed by the manufacturer. The chromagen used for color development was 3,3′-diaminobenzidine, and sections were counterstained with hematoxylin. For the APP antibody only, the biotinylated secondary antibody (1:8000; Vector Laboratories) was followed by incubation with avidin-conjugated alkaline phosphatase, and the McGadey reagent (nitroblue tetrazolium and 5-bromo, 4-chloro, 3-indolyl phosphate) was used for color development with nuclear fast red counterstain. Pretreatments, primary antibody dilutions, and incubation conditions are shown in Table 1. All antibodies labeled specific cell populations or damaged axons (amyloid precursor protein; APP) as described in the literature (Kawarabayashi et al., 1991; Sherriff et al., 1994; Stone et al., 1999). The specificity of the β2 microglobulin (β2m) antibody was confirmed in B6.129P-B2m$^{tm/unc}$ mice (Jackson Laboratories), which do not express β2m. Negative controls in each immunohistochemical experiment consisted of omission of the primary antibody.

Statistics

For parametric values we calculated mean ± SEM and for scores we report the median. To compare hilar cell counts we performed unpaired *t* tests. The nonparametric tests used to compare scores are indicated in the text. Graphpad Prizm was employed for all statistical comparisons.

Results

Behavior during SE and spontaneous seizures

Within a few minutes of pilocarpine injection in CF1 mice, immobility, staring, Straub tail, head bobbing, and occasional clonic seizures occurred, followed after 20–40 min by continuous clonic seizures. If continuous clonic seizures started earlier in CF1 mice, the animal invariably died. SE consisted mainly of continuous stage 3, 3.5, or 4.5 seizures and occasional isolated events of stage 5 and 6 seizures. Typically, seizures became less frequent about 5–6 h after pilocarpine injection. Due to the gradual decrease of seizure activity, the duration of SE could not be determined behaviorally. Moreover, although most behavioral seizures end after 5–6 h, electroencephalograms in pilocarpine-injected mice reveal high-frequency, high-amplitude spiking for about 10 h and the EEG pattern does not become normal for up to 3 days (Kris Bough, personal communication). Thus, similar to Shibley and Smith (2002), we estimated the severity of SE by counting the number of stage 5 and 6 seizures during SE, because they were the most unequivocally and easily identified.

Out of 80 pilocarpine-injected CF1 mice, 26 mice (33% of total) exhibited SE lasting 4–6 h and survived. Mice were euthanized at different times for neuropathological assessment (four mice at 6 h, five at 1 day, six at 3 days, four at 10 days, and seven at 31 days). Twenty-one mice (26% of total) died during or shortly after SE. Thirty-three mice (41%) did not develop SE but only showed intermittent stage 1–3 seizure activity for about 30–60 min. Six of those mice were analyzed neuropathologically, four mice at 3 days and two at 31 days. In all neuropathological evaluations, we found no differences between uninjected mice and pilocarpine-injected mice that did not develop SE (see be-

low). Mice that did not exhibit SE upon the first injection could not be induced by additional pilocarpine (up to 232 mg/kg within 60–90 min of initial injection).

CF1 mice that experienced SE were less active than control mice and ceased nest building (up to 31 days), although they showed no other signs of illness. All seven CF1 mice that experienced SE and were monitored for SRS showed spontaneous seizures during the observation period 17 to 27 days after SE. Often we observed two spontaneous seizures within one 10- to 30-min period and one mouse seized 10 times at 6- to 60-min. intervals in 1 day of observation. Over a 50-h total observation time between day 17 and 27, we observed 1–11 behavioral seizures in each mouse (mean ± SEM 0.08 ± 0.072 seizures/h of observation). In addition, most mice, including mice with just 1 observed spontaneous seizure, had 1 or 2 handling-induced seizures between 11 and 25 days.

CF1 mice: hippocampal cell death and extent of SE

Hematoxylin-stained paraffin sections were assessed for cell loss at the midlevel hippocampus after pilocarpine-induced SE. In five uninjected mice and four pilocarpine-injected mice without SE, no significant pyramidal or granule cell damage was found at 3–31 days (all scores = 0; Fig. 1A1–A3), and there was no significant difference in the number of healthy hilar neurons between the two groups ($p > 0.29$ by unpaired t test). In these mice there were 13.9 ± 1.0 hilar neurons per hippocampal section ($n = 9$), whereas in mice that had experienced SE we counted 0.062 ± 0.026 healthy hilar neurons per section ($n = 26$, $p < 0.0001$ by unpaired t test, Fig. 1B3), including all four mice at 6 h in which no healthy neurons could be found (Fig. 1D). Thus, >99% hilar cell loss was found as early as 6 h after SE.

Varying degrees of pyramidal cell injury, as judged by the presence of shrunken, pyknotic cells (Fig. 1B2, arrowheads) or frank loss of cells (Fig. 1C), were observed at all time points after 6 h. The amount of damage in the pyramidal cell layers was scored in all mice 1–31 days after SE and was symmetrical ($n = 17$, $p > 0.05$ for CA3 and CA1 area scores; Friedman test followed by a Dunn's multiple comparison test). The damage varied considerably between mice, with damage scores ranging from 0.75 to 4 corresponding to >75% to <25% remaining healthy neurons (median score 3.0; $n = 22$). The pyramidal cell damage was not statistically different at different times of euthanasia (Kruskal–Wallis test, $p > 0.07$; also compare different symbols in Fig. 1E and F). These results do not exclude a minor amount of delayed cell death as described in rat with lithium/pilocarpine (Peredery et al., 2000). Examples of minimal and most severe damage are shown in Fig. 1B and C. In most mice (17 of 22) damage was homogenous among CA1 subregions; in the other 5 mice there was no consistent pattern. In the CA3 subsectors, damage was often (18 of 22 mice) less severe in the CA3d area compared to CA3a–c (Wilcoxon matched-pairs signed rank test, $n = 22$, $p < 0.01$). Cell loss in CA1 was usually less than in CA3 (Fig. 1B1 and E), indicating that the CA3 pyramidal cell layer is more sensitive to pilocarpine-induced neurodegeneration in the mouse (Wilcoxon matched-pairs signed rank test, $n = 22$, $p < 0.01$). To investigate whether the amount of pyramidal damage is dependent on the severity of SE, we counted the number of stage 5 and 6 seizures during SE in all 1- to 31-day mice. Mice experiencing fewer than six stage 5–6 seizures showed various degrees of pyramidal cell loss, whereas mice with more than eight stage 5–6 seizures invariably showed severe pyramidal cell loss (Fig. 1F). Consistent with previous reports (Mello et al., 1993; Shibley and Smith, 2002), there was no strong correlation between the extent of pyramidal cell damage and the number of observed SRS in the seven 31-day mice ($r^2 = 0.124$, $p > 0.43$). Only a few mice were observed with obvious pyknotic dentate granule cells: two of six CF1 mice euthanized at 3 d and one C57BL/6 (JAX) mouse at 37 d after SE. The percentage of pyknotic granule cells in these three mice was between 30 and 50%.

Neuronal loss was not restricted to the hippocampus but was found in many other brain areas at early time points after SE. In all mice damage in the thalamus was pronounced, but cell loss also occurred in piriform cortex, striatum, and amygdala.

Neuropeptide Y

Neuropeptide Y is upregulated after seizures in rodents (e.g., Vezzani et al., 1999b) and NPY expression in the supragranular layer of the dentate gyrus reflects mossy fiber sprouting in rats (Scharfman et al., 1999). To assess mossy fiber sprouting, NPY immunohistochemistry has a methodological advantage over Timm's staining because it does not require special perfusion of the animals and can be performed in paraffin sections used for other studies in the same animal. We studied the time course of NPY expression in the CF1 pilocarpine model. In uninjected mice and mice injected with pilocarpine that did not develop SE, NPY immunoreactivity was found in interneurons throughout the hippocampus, including the hilus (Fig. 2B, arrowheads) and in fibers throughout the hippocampus, including the temporoammonic perforant pathway Fig. 2A, arrows) but not the mossy fiber pathway. As early as 6 h after SE, hilar NPY-positive interneurons were lost (not shown). In the mossy fiber pathway, NPY IR was not present in control mice or at 6 h but appeared at 1–31 days after SE in all mice (Fig. 2C–H, arrows). Supragranular NPY labeling in the dentate gyrus became apparent in two of four animals at 10 days (Fig. 2F shows an example without supragranular IR) and in all mice 31 d after SE (e.g., Fig. 2G and H, arrowheads), indicating mossy fiber sprouting.

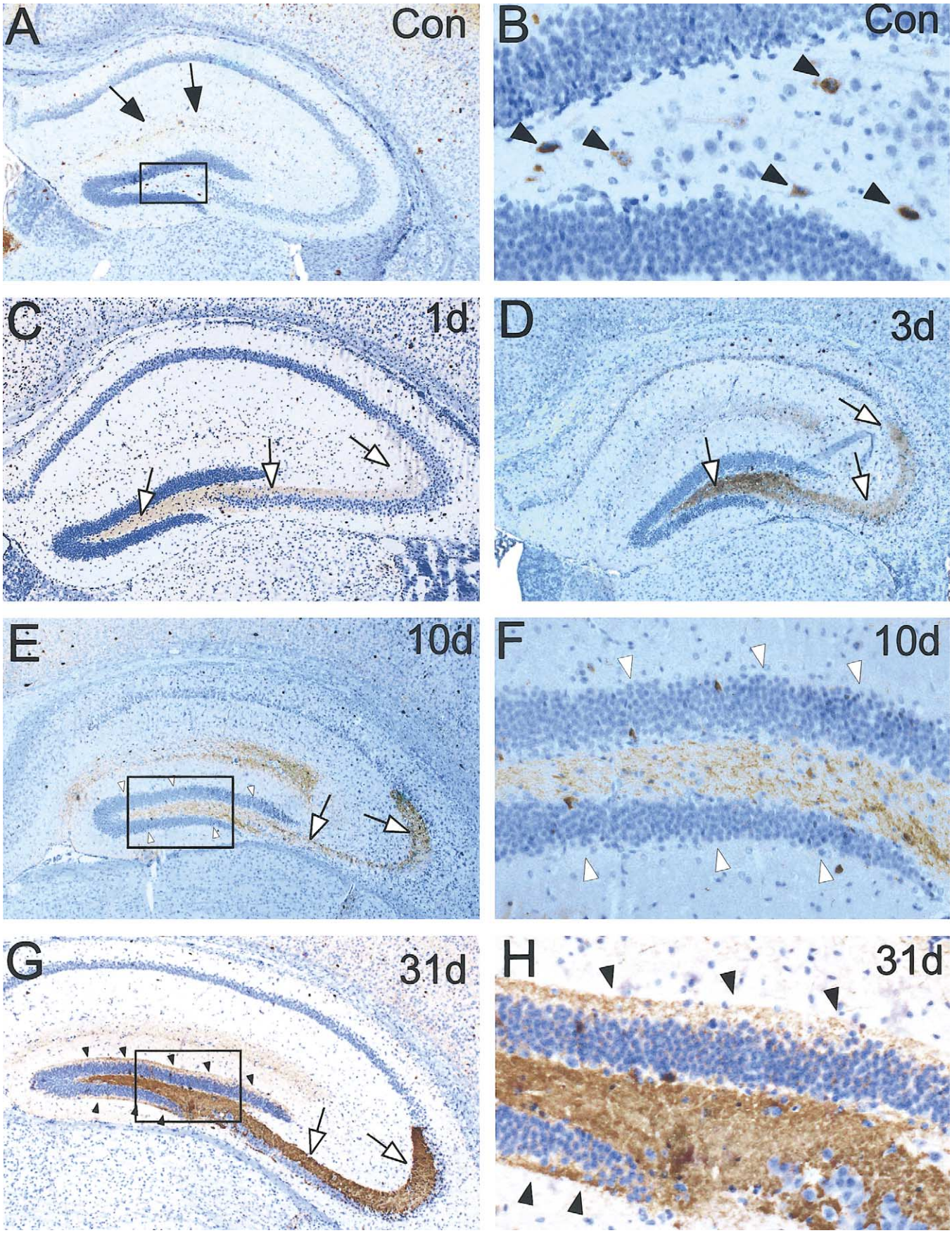

Fig. 2. Persistent NPY upregulation in the mossy fiber pathway after SE. (A and B) Sections of an uninjected mouse showing NPY IR (brown) in the temporoammonic pathway (A, arrows) and in interneurons, e.g., in the hilus (B, arrowheads, counterstained with hematoxylin). (C–H) Sections at different time points after SE (indicated in the upper right corner) revealing NPY IR in the mossy fiber pathway (C–E and G, white arrows), which is absent in control mice. (E and F) In these sections at 10 days, supragranular NPY IR is not found (E and F, white arrowheads), but it appeared at 31 days (G and H, black arrowheads), indicating mossy fiber sprouting.

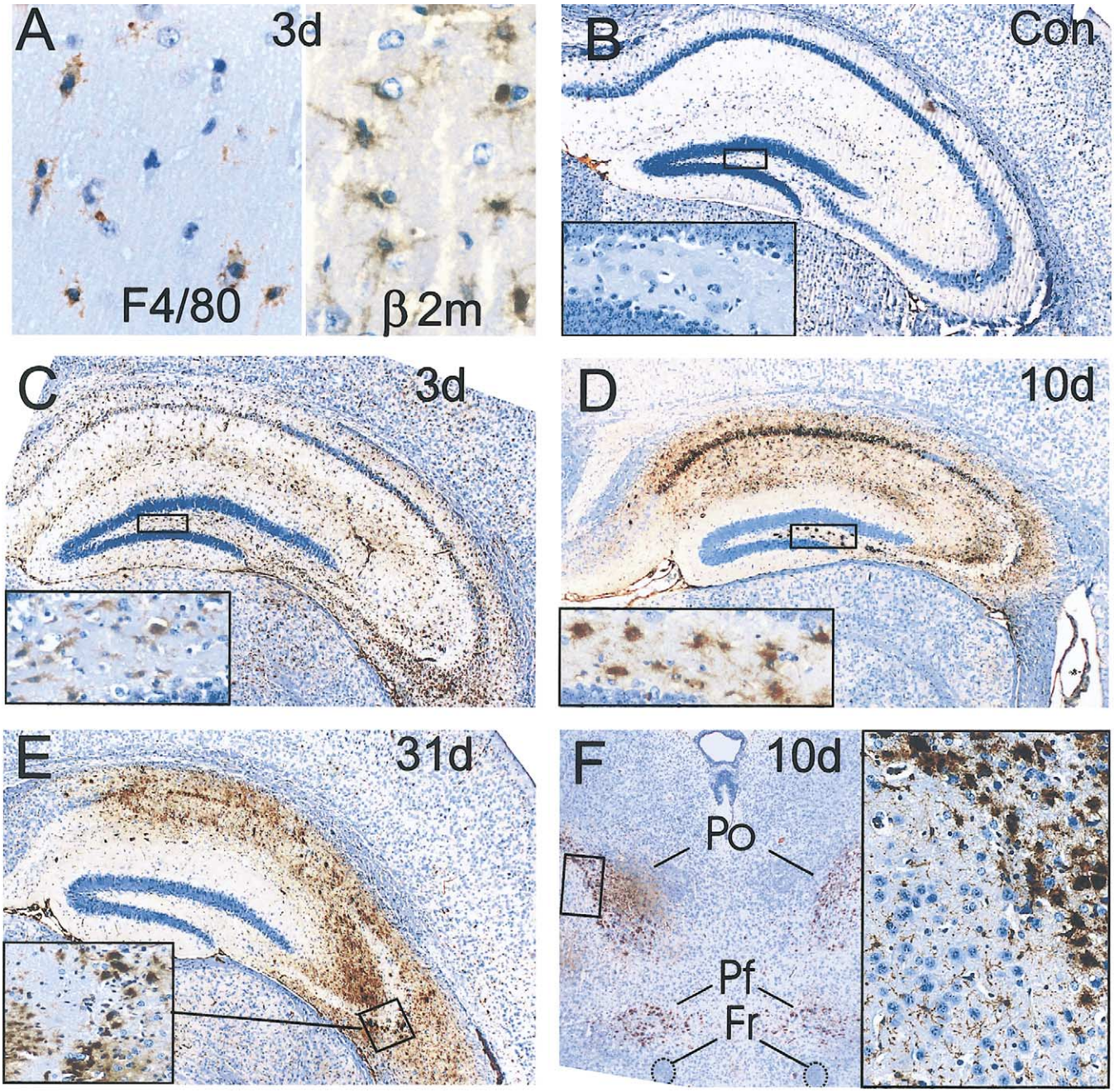

Fig. 3. Activated microglia after SE visualized by β2 microglobulin immunohistochemistry. (A) Immunostaining (brown) with the F4/80 antibody is compared to β2 microglobulin staining at 3 days in the CA1 stratum radiatum, showing IR cells with similar morphology (counterstaining: hematoxylin). (B) A section of an uninjected mouse reveals no significant β2*m* labeling (brown) in the hippocampus and hilus (inset). (C–E) Hippocampal sections at 3 to 31 days show widespread β2m IR in bushy cells (C, E, and F, inset) and phagocytic/ameboid cells (D, E, and F, inset). (F) At 10 days thalamic nuclei, specifically the posterior complex of the thalamus (Po, inset) and the parafascicular nucleus (Pf), exhibit many phagocytic/ameboid microglia (inset). Fr, fasciculus retroflexus.

Microgliosis

Many conventional immunocytochemical markers for microglial cells, such as isolectin B4, F4/80, and CD68, were either unspecific or did not label well in our mouse paraffin sections. F4/80 antibody, an established microglial marker (Andersson et al., 1991), faintly labeled cells with microglial morphology at 3 days after SE (Fig. 3A), but also labeled cells with astrocyte morphology at 10 days (not shown). Microglial cells are also known to express MHC class I and II molecules, especially when activated. Antibodies directed against β2 microglobulin, an MHC class I molecule, labeled a population of cells with typical microglial morphology at 3 days after SE, i.e., bushy cells with

small oval dark nuclei (Fig. 3A and C). We chose to use the β2m antibody to visualize microglia, because robust and reliable staining was obtained in paraffin sections. At all time points after SE (1–31 days), all mice showed β2m IR in cells with microglial morphology, whereas in uninjected mice and injected mice without SE, β2m staining was virtually absent (Fig. 3B). In the hippocampus only a few bushy/ramified faintly β2m-positive cells were observed at 1 day after SE (not shown), but many cells with strong β2m IR were found at 3 days in all mice (Fig. 3C). β2m IR in individual cells increased from 1 to 10 days after SE, especially in the hippocampus, becoming very intense at 10 days, when in all mice bushy and phagocytic/ameboid cells were found in the hilus, stratum radiatum of CA3, and areas with pyramidal cell damage (Fig. 3D). The number of β2m IR cells seemed to depend largely on the size of the damaged areas at 3–10 days. At 31 days, four epileptic mice had lost all or most β2m IR in the hippocampus, whereas three mice continued to exhibit many bushy and phagocytic/ameboid β2m-positive cells in damaged pyramidal cell areas, but not in the hilus (Fig. 3E).

Brain areas other than the hippocampus showed a similar time course of β2m IR. One day after SE in all four examined mice only the thalamic reticular nucleus contained several β2m-positive cells. β2m-positive cells were found throughout the brain in the following brain regions in all mice examined at 3 days ($n = 3$–5) and 10 days ($n = 4$): thalamus, amygdala, piriform cortex, and striatum (only 3 of 4 10-day mice). In thalamic nuclei, most β2m-positive cells had round or oval cell bodies with short stout processes and dark β2m staining, corresponding to phagocytic or ameboid cells (Fig. 3F). At 10 days, strong IR was also found in entorhinal and perirhinal cortex ($n = 4$) and striatum (3 of 4 mice). All seven 31-day mice contained microglia in various thalamic nuclei, striatum, and amygdala and in the piriform area.

Astrogliosis

In uninjected mice and mice injected with pilocarpine that did not develop SE, we observed light GFAP IR in thin astrocyte processes all over the hippocampus (Fig. 4A and B). In all mice at 10 and 31 days after SE, damaged areas, including the hippocampus (Fig. 4C and D) and several thalamic nuclei (Fig. 4E), showed strong GFAP labeling in thickened processes, indicating astrogliosis. The number of healthy neurons was low in areas with strong GFAP expression (Fig. 4G).

Amyloid precursor protein marks axonal damage

APP has been used as a marker for axonal damage in humans and rodents (Kawarabayashi et al., 1991; Sherriff et al., 1994; Stone et al., 1999). In uninjected mice and injected mice without SE only faint APP staining was found around pyramidal cells and other neuronal cell bodies throughout the brain (Fig. 4I, also see 4H, arrowheads). At 10–31 days after SE, strong punctate APP IR appeared in all mice in several thalamic nuclei, including the ventromedial, lateral dorsal, lateral geniculate (dorsal part), central medial and parafascicular nuclei, as well as in the posterior complex of the thalamus and the nucleus reuniens (Fig. 4F and H). The staining was diffuse, punctate, and not associated with cell bodies, indicating axonal labeling (Fig. 4H). Moreover, in some mice at 10–31 days, punctate axonal APP IR was also seen in the nucleus accumbens, amygdala, and piriform areas, including the endopiriform nucleus (not shown). Parallel sections stained with hematoxylin, GFAP, or β2m revealed that areas exhibiting axonal APP IR contained some activated and phagocytotic microglia, many reactive astrocytes, and fewer healthy neuronal cell bodies than adjacent normal areas (Fig. 4G). Moreover, neuronal damage was observed in several thalamic nuclei at 1–3 days. Thus, it appears that axonal injury occurred in areas with earlier damage to neuronal somata. Since APP typically appears in axons as early as 3 h after injury (Kawarabayashi et al., 1991) and we did not observe any APP IR at 1–3 days, we conclude that axonal injury during epileptogenesis is delayed.

Mortality after pilocarpine varies in C57BL/6 mice from different suppliers

Many mouse mutants are available in the C57BL/6 (JAX) strain. Thus, we evaluated the pilocarpine chronic epilepsy model in this strain. Similar to CF1 mice, C57BL/6 (JAX) mice developed SE 30–60 min after pilocarpine injection and continued to exhibit stage ≥3.5 seizures up to 4.5 h until pentobarbital was injected. However, we obtained only 12 C57BL/6 (JAX) mice surviving SE out of 99 pilocarpine-injected mice; 63 mice died, typically within 2 h after pilocarpine injection, and 24 mice did not reach SE, even though we used mice of various ages (6–15 weeks, and over 1-year-old retired breeders), sources (directly shipped from Jackson Laboratories or JAX mice bred in our own facility), and weights (17–32 g), as well as a range of pilocarpine doses (247–335 mg/kg). Nine of the surviving C57BL/6 (JAX) mice with SE were studied neuropathologically at 2 to 37 days after SE (2, 4, 14, 19, and 37 days). Only mice that experienced severe SE of more than 2 h including stage 5 and 6 seizures showed hilar cell loss and upregulation of NPY in the mossy fiber pathway ($n = 5$) or faint supragranular NPY expression after 14 d (Fig. 5C). Two mice in which SE was terminated after 1 h by pentobarbital injection showed no NPY upregulation or obvious hippocampal pyramidal cell or hilar cell loss at 2–3 days, indicating that more than 1 h of SE is necessary to induce cell death and NPY upregulation. In mice with at least 2 h of SE, hilar neuronal loss was >98% ($n = 7$) and various degrees of pyramidal cell loss were found (scores ranged from 0 to 4 with median of 4; $n = 7$). In the hippocampus

reactive microglia were detected after 4 days (Fig. 5A) and gliosis after 14 days (Fig. 5B), and in the thalamus axonal APP IR was found in two mice at 14 and 37 days (Fig. 5D). During 34 h of observation one mouse euthanized at 37 days experienced three spontaneous seizures (0.088 seizures/h).

In contrast to C57BL/6 (JAX) mice, a larger percentage (58%) of C57BL/6 (Charles River) mice developed SE and survived (15 of 26 mice total). Surprisingly, within minutes after the pilocarpine injections C57BL/6 (Charles River), mice experienced continuous whole body clonic seizures (stage 3.5 and 4.5) that continued for about 1 h and then became more intermittent until pentobarbital was administered at 4.5 h. Neuropathological changes in the 11 C57BL/6 (Charles River) mice examined after 2–66 days of SE (2, 3, 5, 8, 9, 65, and 65 days) were similar to those found in CF1 and C57BL/6 (JAX) mice. This includes >97% loss of hilar neurons ($n = 11$), various degrees of pyramidal cell loss (scores ranging from 0.5 to 4, median 2.0; $n = 11$), NPY upregulation in the mossy fiber pathway at all time points (2–66 days), NPY IR in the supragranular layer at 65–66 days, hippocampal gliosis after 8 days, and axonal APP IR in the thalamus at 8–66 days. Many β2m-positive cells were found at 5–9 days in the hippocampus, but β2m-positive cells were scarce or absent in the hippocampus of mice euthanized at 65–66 days. These three mice also exhibited little hippocampal pyramidal cell death (scores: 0.5, 1, and 1), but all three of them showed SRS during 32–39 h of observation time (0.051–0.063 seizures/h).

Discussion

Our principal findings with the mouse pilocarpine model are (1) upregulation of NPY in the mossy fiber pathway beginning 1 day after pilocarpine and at 31 days in the supragranular layer, indicating mossy fiber sprouting; (2) widespread microglial activation detected by β2-microglobulin expression, evident 3 days after SE and persisting in some areas as late as 31 days, suggesting delayed neuronal damage; (3) delayed axonal degeneration visualized by APP-positive fibers particularly in thalamic nuclei; (4) variable cell death in the CA3 and CA1 pyramidal layer not well correlated with the development of spontaneous seizures; (5) hilar neuronal loss, mossy fiber sprouting, and at least some damage in the CA3 pyramidal cell layer area in all epileptic mice; and (6) substantial differences in mortality rate of C57BL/6 mice depending on supplier. In summary, widespread neuropathological changes in neurons and glia were observed after pilocarpine-induced SE, but which changes contribute to or attempt to counter epileptogenesis remain unclear.

Susceptibility to pilocarpine

The genetic background of mice influences their susceptibility to seizure induction by kainate or electroshock, with C57BL/6 mice being among the least susceptible (e.g., Frankel et al., 2001; Schauwecker, 2002). After bilateral carotid occlusion C57BL/6 mice had the highest mortality among seven mouse strains (Yang et al., 1997). We found a striking difference in mortality of C57BL/6 mice from Charles River (low mortality) or Jackson Laboratories (high). It is likely that C57BL/6 mice that have been inbred for decades by different suppliers exhibit genetic differences that underly differential susceptibility. Thus, it is possible that the pilocarpine dose needed to induce SE is closer to the lethal dose in C57B/L6 (JAX) than in C57BL/6 (Charles River) mice.

Neuronal pathology

Pilocarpine-induced SE in the mouse induces widespread neuronal death, NPY upregulation in the mossy fiber pathway, delayed thalamic axonal injury, and mossy fiber sprouting. Neuronal loss is a common feature in human epilepsies and most rodent epilepsy models, including a mouse model of mesial temporal lobe epilepsy induced by intrahippocampal kainate injection (Bouilleret et al., 1999; Suzuki et al., 1995), in which cell loss is limited to the hippocampus and not as widespread as in the pilocarpine model. Neuronal injury typically precedes the occurrence of spontaneous seizures, however, it is unclear whether the extent of cell loss is linked to the onset or frequency of spontaneous seizures. In some models there is positive correlation between extent of cell death and SRS onset or frequency. For example, Mello et al. (1993) showed a correlation between the remaining CA3 pyramidal cell density and the time to SRS onset after pilocarpine-induced SE in rats. In our hands, however, the extent of damage in the hippocampal pyramidal cell layer varied extensively among mice and was not correlated to the occurrence of SRS, although we examined only seven CF1 and four C57BL/6 mice with SRS. Similarly, a chronic rat epilepsy model was described recently in which neuronal death could not be detected (Zhang et al., 2002). In this study rats were primed twice by brief kainate-evoked seizures before prolonged SE was induced with pilocarpine or kainate; primed rats exhibited a similar onset and frequency of SRS as nonprimed rats with SE and cell loss.

The loss of hilar neurons has been described in human temporal lobe epilepsy (e.g., Magloczky et al., 2000 and review by Houser, 1992), in many epilepsy models (Ben-Ari, 1985; Buckmaster and Dudek, 1997), including the pilocarpine rat model (Mello et al., 1993) and the mouse model of mesial temporal lobe epilepsy (Bouilleret et al., 2000), and appears to be a better indicator for the development of SRS in nonprimed rodent models. In our hands, mice from different strains that experienced pilocarpine-induced SE and also exhibited severe hilar cell loss all experienced SRS. In contrast, strong, prolonged (4 h) SE caused by repeated injection of kainate in CF1 mice produced no significant hilar cell loss and no spontaneous

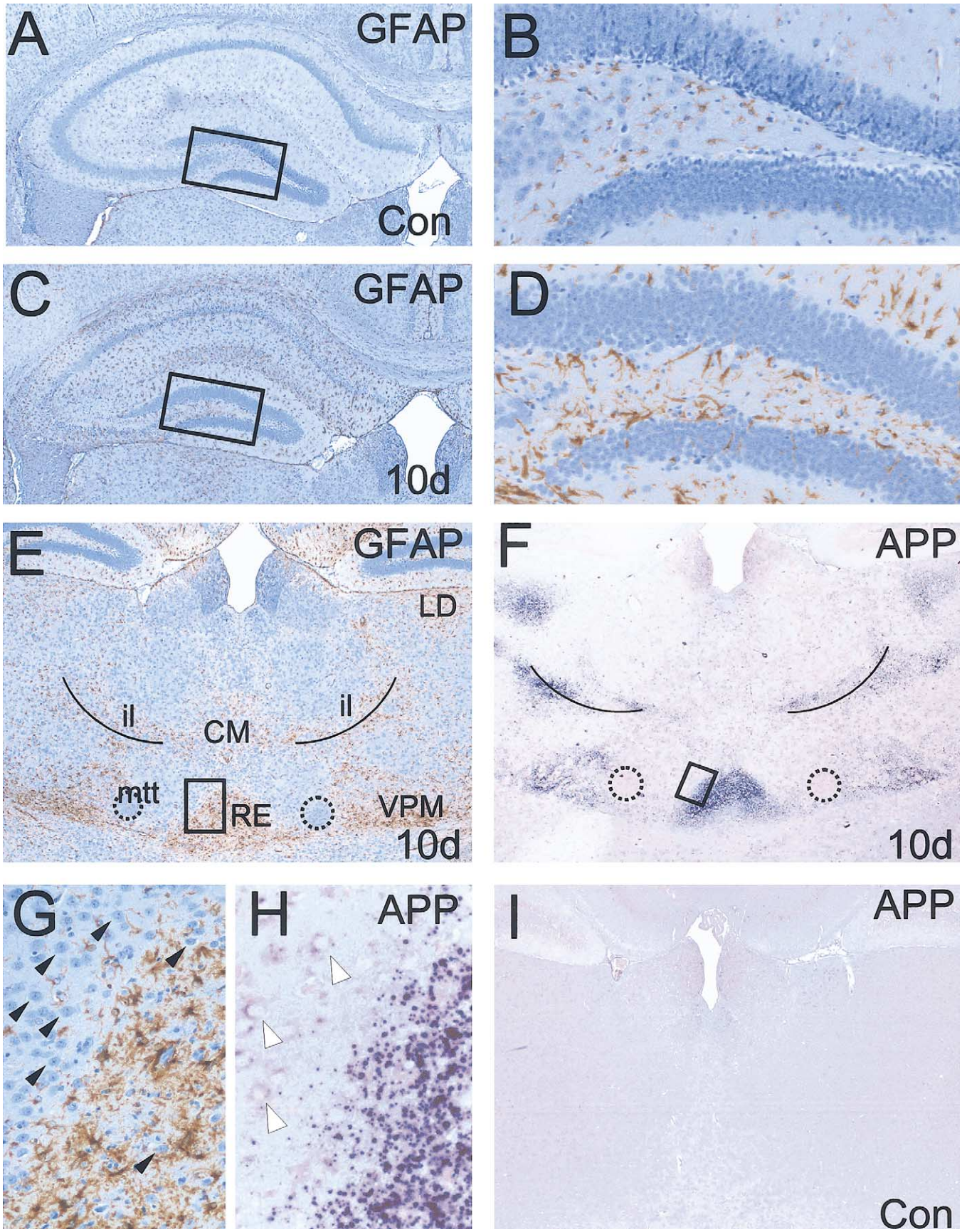
A
GFAP
Con
B
C
GFAP
10d
D
E
GFAP
LD
il
CM
il
mtt
RE
VPM
10d
F
APP
10d
G
H
APP
I
APP
Con

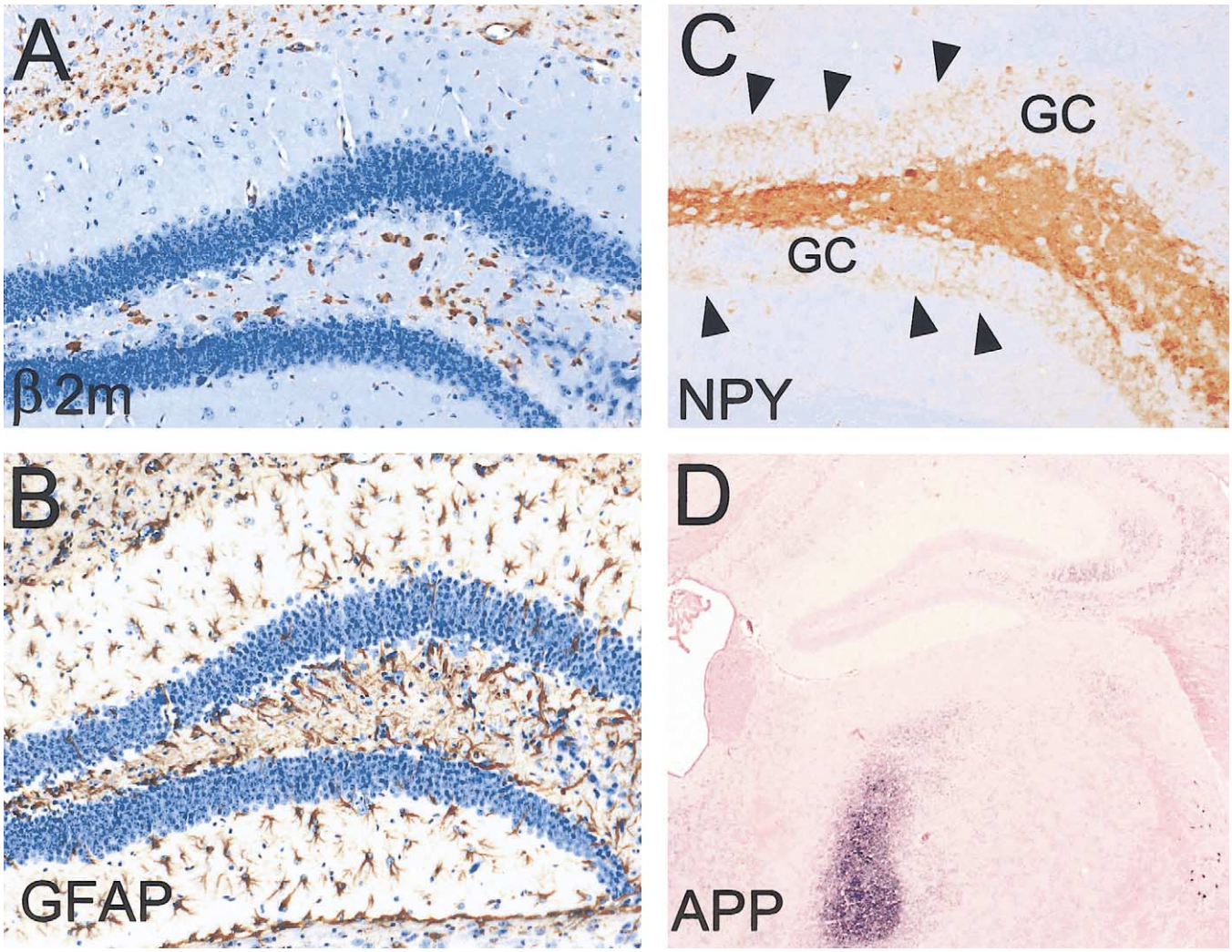

Fig. 5. Neuropathology of a C57BL/6 (JAX) mouse 14 days after SE. Immunostainings (brown) of the hilus for β2 microglobulin (A) revealing phagocytic/ameboid microglia and for GFAP (B) revealing gliosis (counterstained with hematoxylin). (C) NPY IR in mossy fibers and faint IR in the supragranular layer (arrowheads; GC, granule cells; no hematoxylin counterstain). (D) Axonal APP IR (blue) in the posterior complex of the thalamus.

seizures during a total of 27 h of observation between 14 and 35 days after SE (data not shown). Gorter et al. (2001) showed that rats that developed progressive epilepsy, in which the frequency of SRS increased over a period of weeks, exhibited bilateral, severe hilar cell loss. In contrast, in nonprogressive rats exhibiting constant SRS frequency over time, extensive hilar cell loss was mainly unilateral, whereas CA3 damage was bilateral in both progressive and nonprogressive rats. Mice lacking the peptide neurotransmitter somatostatin, which is found in many dentate and hilar interneurons that are lost in epilepsy models, showed more severe seizures than wild-type mice (Buckmaster et al., 2002). Finally, focal ablation of interneurons containing substance P receptors, including hilar neurons but without loss of principal cells in the hippocampus, produced hyperexcitability in the adjacent dentate granule cell and CA1 pyramidal layer, but whether rats developed SRS was not examined (Martin and Sloviter, 2001). In conclusion, the loss of hilar neurons but not hippocampal pyramidal cells may correlate with the development of SRS or progressive-

Fig. 4. Astrogliosis and axonal damage at 10 days after SE. (A and B) Sections of an uninjected mouse with little GFAP IR (brown) in the hippocampus (A), including the hilus (B). At 10 days after SE increased GFAP IR in the hippocampus and hilus (C and D) and in many thalamic nuclei (E) was seen. (F) APP IR in a parallel section to E. Parts of the nucleus reuniens (RE, boxed in E and F) are shown at higher power containing many GFAP IR astrocytes (G), but few healthy appearing neuronal cell bodies relative to the nongliotic area (G, arrowheads), and strong punctate APP IR (H). Arrowheads in H show neuronal cell bodies surrounded by light APP IR, which are also seen in mice without SE (not shown). (I) A representative uninjected mouse stained with APP is devoid of blue punctate IR. A: LD, lateral dorsal nucleus; VPM, ventralposteromedial nucleus; RE, nucleus reuniens; CM, central medial nucleus of the thalamus; mtt, mammillothalamic tract.

ness in nonprimed induced epilepsy models. However, loss of hilar neurons is usually also associated with gliosis and mossy fiber sprouting. Thus, it remains to be determined whether hilar neuron loss can induce epilepsy by itself or whether secondary changes such as gliosis or mossy fiber sprouting are necessary.

Another interesting persistent neuronal change commencing 1 day after pilocarpine-induced SE was NPY expression in the mossy fiber pathway. NPY has long been known to be induced in mossy fibers shortly after seizures induced by kainate, hilar lesion, or kindling (reviewed in Vezzani et al., 1999b) and at late time points after SE induced by electrical stimulation (Schwarzer et al., 1995) or pilocarpine (Scharfman et al., 1999). In genetically epileptic rodents (e.g., Chafetz et al., 1995), NPY is upregulated and, furthermore, the number and length of NPY-positive fibers was increased in human temporal lobe epilepsy (Furtinger et al., 2001). However, to our knowledge this is the first report showing that NPY is persistently upregulated at different time points in a rodent pilocarpine model. In addition, mice lacking NPY show unusually high mortality after kainate-induced seizures (Baraban et al., 1997), whereas rats overexpressing NPY are less susceptible to kainate-induced seizures and kindling (Vezzani et al., 2002). Many findings from other seizure models, mutant mice, and humans, suggest that NPY upregulation in mossy fibers and the regulation of NPY receptor levels tends to suppress the development of seizures (see Furtinger et al., 2001 and review by Vezzani et al., 1999b).

APP immunohistochemistry is a common tool to assess axonal injury in humans and animals, because APP accumulates in axons early after injury presumably due to impaired axonal transport (Kawarabayashi et al., 1991; Sherriff et al., 1994; Stone et al., 1999). Using APP immunohistochemistry, we found delayed axonal damage (after 8–10 days) in many thalamic nuclei, amygdala, and piriform cortex, which may be due to injury of the neurons themselves or may have been induced secondarily by earlier loss of their target neurons. In agreement with our observations, Kawarabayashi et al. (1991) observed APP IR in axons up to 60 days after kainate injection in rats. In humans, axonal damage visualized by APP IR was also found in about 60% of cases in which SE caused by various conditions led to death within 6 h to 8 days (Dolinak et al., 2000). Interestingly, in two of three patients that experienced SE and had epilepsy, no axonal death was observed, and similarly, in surgically removed epileptic tissue from temporal lobe epilepsy patients, APP IR has not been found in dystrophic neurites to our knowledge (e.g., Sheng et al., 1994). These results taken together suggest that the observed axonal damage in pilocarpine-treated mice is caused by SE itself rather than by secondary, briefer seizures.

In the rat pilocarpine epilepsy model, thalamic nuclei are activated during SE (Barone et al., 1993). Prominent thalamic degeneration occurs in the rat and mouse pilocarpine model as well as in the rat kainate model (Covolan and Mello, 2000; Turski et al., 1983, 1984). Thalamic injury was also reported in some human temporal lobe epilepsy cases as judged by magnetic resonance imaging (Deasy et al., 2000), although no obvious thalamic damage has been described after intrahippocampal kainate injection in mice, which leads to development of epilepsy (Bouillerret et al., 1999). Notably, many of the thalamic nuclei affected do not belong to the limbic system but to the thalamo–striatal–cortical system or the central autonomic system. Traditionally, the thalamic–striatal system was thought *not* to play a role in limbic seizures but rather to induce absence seizures (see discussion in Mraovitch and Calando, 1999). However, Mraovitch and Calando (1999) showed that stereotaxic carbachol injection into thalamic nuclei of the thalamo–striatal–cortical system induced limbic and generalized convulsive seizures and activated the limbic and central autonomic system as detected by *c-fos* immunohistochemistry. Thus, further investigation of the role of the thalamo–striatal–cortical and the central autonomic system in epilepsy is warranted, because disruption of mechanisms involved in adaptive homeostatic responses might contribute to hyperexcitability and degeneration in limbic pathways.

Glial activation

Glial changes observed in the pilocarpine mouse model include widespread microglial activation and persistent astrogliosis in areas with neuronal damage; such gliosis has been observed in many epilepsy models and human temporal lobe epilepsy. Both microglial and astroglial activation typically follow neuronal damage and can promote tissue repair but might also contribute to epileptogenesis.

Microglial cells, the principal immune cells of the brain, have a critical role in the defense of the brain against infectious diseases, inflammation, trauma, ischemia, brain tumors, and neurodegeneration. Neuronal damage rapidly activates microglia in their immediate vicinity. Activated microglia are phagocytic, destroying invading microorganisms and removing potentially deleterious debris. They also secrete neuronal growth factors that might promote neural tissue repair. However, there is evidence that microglia may exert not only neurotrophic but also neurotoxic effects (Aschner et al., 1999; Hanisch, 2002; Rogove and Tsirka, 1998). Because reactive microglia can be present for a prolonged time in epileptic mice and are found in human sclerotic hippocampi after lobectomy from temporal lobe epilepsy patients (Beach et al., 1995), it is conceivable that activated microglia could promote seizures, for example, by secreting the proinflammatory interleukin-1β. Supporting this suggestion are the observations that microglia secrete interleukin-1β after seizures, interleukin-1β increases seizure susceptibility in rodents and man (reviewed in Jankowsky and Patterson, 2001), and intracerebral injection of interleukin 1β prolongs kainate-induced seizures (Vezzani et al., 1999a).

During the last 20 years many new functions of astro-

cytes, in addition to spatial buffering of potassium and structural roles, have been revealed. Astrocytes can secrete extracellular matrix molecules and growth factors that influence neuronal survival and axonal and dendritic sprouting (reviewed in Barres and Barde, 2000); they can promote synapse formation, maintain synaptic function by taking up synaptically released glutamate, and might actively modulate synaptic function (Pfrieger and Barres, 1996). For example, glutamate-stimulated astrocytes in culture can release D-serine, an agonist at the NMDA receptor glycine site (Schell et al., 1995). Shortly after seizures, astrocytes release several cytokines and growth factors such as the neuroprotective basic fibroblast growth factor, leukocyte inhibitory factor, which seems to be involved in upregulation of GFAP mRNA after seizures (Jankowsky and Patterson, 2001), and interleukin-6, which has been implicated in inducing microgliosis and astrogliosis (Penkowa et al., 2001).

Taken together, the observed pathology after pilocarpine-induced SE in the mouse makes it likely that both glial and neuronal changes contribute to epileptogenesis. Thus, new therapeutic approaches targeting glial cells in addition to neurons to inhibit epileptogenesis are worth considering.

Acknowledgments

This study was supported by grants from the Emory University research council (K.B.), the Epilepsy Foundation (K.B.), and the NINDS (NS17771). We are grateful to Dr. David Rye for help with identification of thalamic nuclei and Robert Baul for excellent technical assistance.

References

Andersson, P.B., Perry, V.H., Gordon, S., 1991. The kinetics and morphological characteristics of the macrophage–microglial response to kainic acid-induced neuronal degeneration. Neuroscience 42, 201–214.

Aschner, M., Allen, J.W., Kimelberg, H.K., LoPachin, R.M., Streit, W.J., 1999. Glial cells in neurotoxicity development. Annu. Rev. Pharmacol. Toxicol. 39, 151–173.

Baraban, S.C., Hollopeter, G., Erickson, J.C., Schwartzkroin, P.A., Palmiter, R.D., 1997. Knock-out mice reveal a critical antiepileptic role for neuropeptide Y. J. Neurosci. 17, 8927–8936.

Barone, P., Morelli, M., Cicarelli, G., Cozzolino, A., DeJoanna, G., Campanella, G., DiChiara, G., 1993. Expression of c-fos protein in the experimental epilepsy induced by pilocarpine. Synapse 14, 1–9.

Barres, B.A., Barde, Y., 2000. Neuronal and glial cell biology. Curr. Opin. Neurobiol. 10, 642–648.

Beach, T.G., Woodhurst, W.B., MacDonald, D.B., Jones, M.W., 1995. Reactive microglia in hippocampal sclerosis associated with human temporal lobe epilepsy. Neurosci. Lett. 191, 27–30.

Ben-Ari, Y., 1985. Limbic seizure and brain damage produced by kainic acid: mechanisms and relevance to human temporal lobe epilepsy. Neuroscience 14, 375–403.

Berkeley, J.L., Decker, M.J., Levey, A.I., 2002. The role of muscarinic acetylcholine receptor-mediated activation of extracellular signal-regulated kinase 1/2 in pilocarpine-induced seizures. J. Neurochem. 82, 192–201.

Bouilleret, V., Loup, F., Kiener, T., Marescaux, C., Fritschy, J.M., 2000. Early loss of interneurons and delayed subunit-specific changes in GABA(A)-receptor expression in a mouse model of mesial temporal lobe epilepsy. Hippocampus 10, 305–324.

Bouilleret, V., Ridoux, V., Depaulis, A., Marescaux, C., Nehlig, A., Le Gal La Salle, G., 1999. Recurrent seizures and hippocampal sclerosis following intrahippocampal kainate injection in adult mice: electroencephalography, histopathology and synaptic reorganization similar to mesial temporal lobe epilepsy. Neuroscience 89, 717–729.

Buckmaster, P.S., Dudek, F.E., 1997. Neuron loss, granule cell axon reorganization, and functional changes in the dentate gyrus of epileptic kainate-treated rats. J. Comp. Neurol. 385, 385–404.

Buckmaster, P.S., Otero-Corchon, V., Rubinstein, M., Low, M.J., 2002. Heightened seizure severity in somatostatin knockout mice. Epilepsy Res. 48, 43–56.

Cavalheiro, E.A., Leite, J.P., Bortolotto, Z.A., Turski, W.A., Ikonomidou, C., Turski, L., 1991. Long-term effects of pilocarpine in rats: structural damage of the brain triggers kindling and spontaneous recurrent seizures. Epilepsia 32, 778–782.

Cavalheiro, E.A., Santos, N.F., Priel, M.R., 1996. The pilocarpine model of epilepsy in mice. Epilepsia 37, 1015–1019.

Chafetz, R.S., Nahm, W.K., Noebels, J.L., 1995. Aberrant expression of neuropeptide Y in hippocampal mossy fibers in the absence of local cell injury following the onset of spike-wave synchronization. Brain Res. Mol. Brain Res. 31, 111–121.

Covolan, L., Mello, L.E., 2000. Temporal profile of neuronal injury following pilocarpine or kainic acid-induced status epilepticus. Epilepsy Res. 39, 133–152.

Deasy, N.P., Jarosz, J.M., Elwes, R.C., Polkey, C.E., Cox, T.C., 2000. Thalamic changes with mesial temporal sclerosis: MRI. Neuroradiology 42, 346–351.

Dolinak, D., Smith, C., Graham, D.I., 2000. Global hypoxia per se is an unusual cause of axonal injury. Acta Neuropathol. 100, 553–560.

Frankel, W.N., Taylor, L., Beyer, B., Tempel, B.L., White, H.S., 2001. Electroconvulsive thresholds of inbred mouse strains. Genomics 74, 306–312.

Furtinger, S., Pirker, S., Czech, T., Baumgartner, C., Ransmayr, G., Sperk, G., 2001. Plasticity of Y1 and Y2 receptors and neuropeptide Y fibers in patients with temporal lobe epilepsy. J. Neurosci. 21, 5804–5812.

Gearing, M., Wilson, R.W., Unger, E.R., Shelton, E.R., Chan, H.W., Masters, C.L., Beyrcuther, K., Mirra, S.S., 1993. Amyloid precursor protein (APP) in the striatum in Alzheimer's disease: an immunohistochemical study. J. Neuropathol. Exp. Neurol. 52, 22–30.

Gorter, J.A., van Vliet, E.A., Aronica, E., Lopes da Silva, F.H., 2001. Progression of spontaneous seizures after status epilepticus is associated with mossy fibre sprouting and extensive bilateral loss of hilar parvalbumin and somatostatin-immunoreactive neurons. Eur. J. Neurosci. 13, 657–669.

Hanisch, U.K., 2002. Microglia as a source and target of cytokines. Glia 40, 140–155.

Hof, P., Young, W.G., Bloom, F.E., Belichenko, P.V., Celio, M.R., 2000. Comparative Cytoarchitonic Atlas of the C57BL/6 and 129/Sv Mouse Brains. Elsevier, New York.

Houser, C.R., 1992. Morphological changes in the dentate gyrus in human temporal lobe epilepsy. Epilepsy Res. Suppl. 7, 223–234.

Jankowsky, J.L., Patterson, P.H., 2001. The role of cytokines and growth factors in seizures and their sequelae. Prog. Neurobiol. 63, 125–149.

Kawarabayashi, T., Shoji, M., Harigaya, Y., Yamaguchi, H., Hirai, S., 1991. Expression of APP in the early stage of brain damage. Brain Res. 563, 334–338.

Magloczky, Z., Wittner, L., Borhegyi, Z., Halasz, P., Vajda, J., Czirjak, S., Freund, T.F., 2000. Changes in the distribution and connectivity of interneurons in the epileptic human dentate gyrus. Neuroscience 96, 7–25.

Martin, J.L., Sloviter, R.S., 2001. Focal inhibitory interneuron loss and principal cell hyperexcitability in the rat hippocampus after microin-

jection of a neurotoxic conjugate of saporin and a peptidase-resistant analog of Substance P. J. Comp. Neurol. 436, 127–152.

Mello, L.E., Cavalheiro, E.A., Tan, A.M., Kupfer, W.R., Pretorius, J.K., Babb, T.L., Finch, D.M., 1993. Circuit mechanisms of seizures in the pilocarpine model of chronic epilepsy: cell loss and mossy fiber sprouting. Epilepsia 34, 985–995.

Mraovitch, S., Calando, Y., 1999. Interactions between limbic, thalamo–striatal–cortical, and central autonomic pathways during epileptic seizure progression. J. Comp. Neurol. 411, 145–161.

Penkowa, M., Molinero, A., Carrasco, J., Hidalgo, J., 2001. Interleukin-6 deficiency reduces the brain inflammatory response and increases oxidative stress and neurodegeneration after kainic acid-induced seizures. Neuroscience 102, 805–818.

Peredery, O., Persinger, M.A., Parker, G., Mastrosov, L., 2000. Temporal changes in neuronal dropout following inductions of lithium/pilocarpine seizures in the rat. Brain Res. 881, 9–17.

Pfrieger, F.W., Barres, B.A., 1996. New views on synapse–glia interactions. Curr. Opin. Neurobiol. 6, 615–621.

Racine, R.J., 1972. Modification of seizure activity by electrical stimulation. II. Motor seizure. Electroencephalogr. Clin. Neurophysiol. 32, 281–294.

Rogove, A.D., Tsirka, S.E., 1998. Neurotoxic responses by microglia elicited by excitotoxic injury in the mouse hippocampus. Curr. Biol. 8, 19–25.

Scharfman, H.E., Goodman, J.H., Sollas, A.L., 1999. Actions of brain-derived neurotrophic factor in slices from rats with spontaneous seizures and mossy fiber sprouting in the dentate gyrus. J. Neurosci. 19, 5619–5631.

Schauwecker, P.E., 2002. Complications associated with genetic background effects in models of experimental epilepsy. Prog. Brain Res. 135, 139–148.

Schauwecker, P.E., Steward, O., 1997. Genetic determinants of susceptibility to excitotoxic cell death: implications for gene targeting approaches. Proc. Natl. Acad. Sci. USA 94, 4103–4108.

Schell, M.J., Molliver, M.E., Snyder, S.H., 1995. D-serine, an endogenous synaptic modulator: localization to astrocytes and glutamate-stimulated release. Proc. Natl. Acad. Sci. USA 92, 3948–3952.

Schwarzer, C., Williamson, J.M., Lothman, E.W., Vezzani, A., Sperk, G., 1995. Somatostatin, neuropeptide Y, neurokinin B and cholecystokinin immunoreactivity in two chronic models of temporal lobe epilepsy. Neuroscience 69, 831–845.

Sheng, J.G., Boop, F.A., Mrak, R.E., Griffin, W.S., 1994. Increased neuronal beta-amyloid precursor protein expression in human temporal lobe epilepsy: association with interleukin-1 alpha immunoreactivity. J. Neurochem. 63, 1872–1879.

Sherriff, F.E., Bridges, L.R., Sivaloganathan, S., 1994. Early detection of axonal injury after human head trauma using immunocytochemistry for beta-amyloid precursor protein. Acta Neuropathol. 87, 55–62.

Shibley, H., Smith, B.N., 2002. Pilocarpine-induced status epilepticus results in mossy fiber sprouting and spontaneous seizures in C57BL/6 and CD-1 mice. Epilepsy Res. 49, 109–120.

Stone, J.R., Walker, S.A., Povlishock, J.T., 1999. The visualization of a new class of traumatically injured axons through the use of a modified method of microwave antigen retrieval. Acta Neuropathol. 97, 335–345.

Suzuki, F., Junier, M.P., Guilhem, D., Sorensen, J.C., Onteniente, B., 1995. Morphogenetic effect of kainate on adult hippocampal neurons associated with a prolonged expression of brain-derived neurotrophic factor. Neuroscience 64, 665–674.

Turski, W.A., Cavalheiro, E.A., Bortolotto, Z.A., Mello, L.M., Schwarz, M., Turski, L., 1984. Seizures produced by pilocarpine in mice: a behavioral, electroencephalographic and morphological analysis. Brain Res. 321, 237–253.

Turski, W.A., Cavalheiro, E.A., Schwarz, M., Czuczwar, S.J., Kleinrok, Z., Turski, L., 1983. Limbic seizures produced by pilocarpine in rats: behavioral, electroencephalographic and neuropathological study. Behav. Brain Res. 9, 315–335.

Vezzani, A., Conti, M., De Luigi, A., Ravizza, T., Moneta, D., Marchesi, F., De Simoni, M.G., 1999a. Interleukin-1beta immunoreactivity and microglia are enhanced in the rat hippocampus by focal kainate application: functional evidence for enhancement of electrographic seizures. J. Neurosci. 19, 5054–5065.

Vezzani, A., Michalkiewicz, M., Michalkiewicz, T., Moneta, D., Ravizza, T., Richichi, C., Aliprandi, M., Mule, F., Pirona, L., Gobbi, M., Schwarzer, C., Sperk, G., 2002. Seizure susceptibility and epileptogenesis are decreased in transgenic rats overexpressing neuropeptide Y. Neuroscience 110, 237–243.

Vezzani, A., Sperk, G., Colmers, W.F., 1999b. Neuropeptide Y: emerging evidence for a functional role in seizure modulation. Trends Neurosci. 22, 25–30.

Yang, G., Kitagawa, K., Matsushita, K., Mabuchi, T., Yagita, Y., Yanagihara, T., Matsumoto, M., 1997. C57BL/6 strain is most susceptible to cerebral ischemia following bilateral common carotid occlusion among seven mouse strains: selective neuronal death in the murine transient forebrain ischemia. Brain Res. 752, 209–218.

Zhang, X., Cui, S.S., Wallace, A.E., Hannesson, D.K., Schmued, L.C., Saucier, D.M., Honer, W.G., Corcoran, M.E., 2002. Relations between brain pathology and temporal lobe epilepsy. J. Neurosci. 22, 6052–6061.